JOURNAL OF MATERIALS SCIENCE 24 (1989) 3521–3528

Layer removal analysis of residual stress

Part 2 *A new procedure for polymer mouldings with depth-varying Young's modulus*

M. W. A. PATERSON, J. R. WHITE
Department of Metallurgy and Engineering Materials, University of Newcastle-upon-Tyne, Newcastle-upon-Tyne NE1 7RU, UK

A method is presented for the analysis of residual stresses in parallel-sided polymer mouldings with depth-varying Young's modulus. The experimental procedure is the same as the layer removal technique developed by Treuting and Read and requires removal of uniform layers from the surface and measurement of the resulting curvature when all external tractions are removed. When the Young's modulus varies with depth, certain of the simplifications made by Treuting and Read are no longer valid, but it is shown here that a satisfactory alternative procedure can be used as long as the modulus distribution is known. Examples of the application of the new procedure are given for an injection-moulded nylon 6, 6 bar stored in dry conditions, in which the modulus rose steeply near to the surface, and another bar, also made from nylon 6, 6, in which exposure to water produced a quite different distribution, with a maximum at the centre.

1. Introduction

Residual stresses form in injection mouldings as a consequence of the thermal gradients that prevail during the solidification process [1–3]. A further contribution to residual stress may result from molecular recoil as molecules that become extended during flow return to a more random conformation. A popular method of measuring these stresses in bar and plaques is to apply a layer removal analysis. Thin uniform layers are machined from one surface and the curvature that is produced to restore force equilibrium is measured at each incremental removal. A plot of curvature against thickness removed can then be used to derive the stress distribution through the thickness of the moulding by a procedure described by Treuting and Read [4]. In this analysis the stresses are assumed to be uniform at a particular depth within the moulding, but biaxial stresses are allowed for; the Young's modulus and Poisson's ratio are taken to be uniform throughout.

Injection mouldings often have a significant depth-dependent variation in stiffness, whether unfilled [5–13] or if they contain short-fibre reinforcement [14, 15], and it has been pointed out that this will lead to errors in the unmodified form of the Treuting and Read analysis [16–18]. To investigate the effect of this in a quantitative manner, the following procedure was developed and appeared as Part 1 [18]. A notional stress distribution (parabolic) and a notional Young's modulus distribution were chosen. The curvatures that would be obtained for successive layer removals from a bar with this combination were then computed. Finally the curvature against depth removed plot generated in this way was used for an unmodified Treuting and Read analysis [4], using the average modulus to represent the "uniform" modulus in their formula which enables the residual stress distribution to be computed from the curvature data. The computed residual stress distribution was then compared with the true (chosen) distribution. The computed distributions obtained for certain modulus distributions are reminiscent of those obtained in some experimental studies, and this was discussed in Part 1 [18]. Although this confirms that modulus variations could account for (some of) the departures of experimental residual stress distributions from those predicted from thermoelastic calculations, it does not provide the means to derive the stress distribution, even if the modulus distribution is known. The purpose of this paper is to present a method for this.

2. Theoretical analysis

Consider a bar, thickness $2z_0$, in which the Young's modulus $E(z)$ varies with depth, and which possesses a residual stress distribution $\sigma_i(z)$. z is measured from the plane located at the bar centre before layer removals commence (referred to later as the reference surface). If a layer is removed, so that the upper surface is now located at $z = z_1$, the bar bends to restore internal force equilibrium (Fig. 1). In the Treuting and Read derivation it is assumed that the modulus is uniform, so that the neutral surface is located at the centre of the reduced bar. When the restriction of uniform modulus is removed, the location of the neutral surface must be computed from

$$\int_{-z_0}^{z_1} (z + w)E_x(z)\,dz = 0 \qquad (1)$$

where w is the distance of the neutral surface from the reference surface (Fig. 1). $E_x(z)$ is the Young's

0022–2461/89 $03.00 + .12

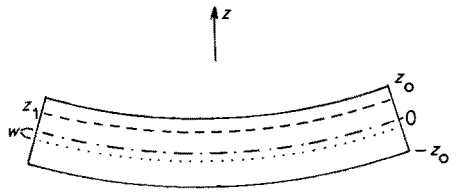

Figure 1 Cross-section of bar with original thickness $2z_0$ with central reference plane at $z = 0$. The bar curves in the sense shown when layers are removed so that the top surface becomes located at $z = z_1$ if the surface stresses are compressive; the neutral surface moves down a distance w (dotted line).

modulus in the x-direction, taken here to be the bar axis direction.

If the residual stress in the x-direction is denoted $\sigma_{ix}(z)$ then the bending moment per unit width about the neutral surface is given by

$$M_x(z_1) = \int_{-z_0}^{z_1} (z + w)\sigma_{ix}\, dz \qquad (2)$$

The next step, as in the Appendix in the paper by Treuting and Read [4], is to differentiate M_x with respect to z_1, noting that z_1 is present in the upper limit of the integral and that w within the integrand is a function of z_1

$$\frac{dM_x}{dz_1} = (z_1 + w)\sigma_{ix} + \frac{dw}{dz_1}\int_{-z_0}^{z_1} \sigma_{ix}\, dz \qquad (3a)$$

or

$$\frac{dM_x}{dz_1} = (z_1 + w)\sigma_{ix} + F_x\frac{dw}{dz_1} \qquad (3b)$$

where F_x is defined, as in [4], as

$$F_x(z_1) = \int_{-z_0}^{z_1} \sigma_{ix}\, dz \qquad (4)$$

By differentiating Equation 1 with respect to z_1 we obtain

$$(z_1 + w)E_x + \frac{dw}{dz_1}\int_{-z_0}^{z_1} E_x\, dz = 0$$

i.e.

$$\frac{dw}{dz_1} = \frac{-(z_1 + w)E_x}{\int_{-z_0}^{z_1} E_x\, dz} \qquad (5)$$

Substituting Equation 5 into Equation 3b and rearranging

$$F_x = \frac{\sigma_{ix}}{E_x}\int_{-z_0}^{z_1} E_x\, dz - \frac{1}{(z_1 + w)E_x}\int_{-z_0}^{z_1} E_x\, dz\left(\frac{dM_x}{dz_1}\right) \qquad (6)$$

From Equation (4) it follows that $dF_x/dz_1 = \sigma_{ix}$, so by differentiating Equation 6

$$\sigma_{ix} = \frac{d\sigma_{ix}}{dz_1}\frac{\int_{-z_0}^{z_1} E_x\, dz}{E_x} + \frac{\sigma_{ix}\left[E_x^2 - \frac{dE_x}{dz_1}\int_{-z_0}^{z_1} E_x\, dz\right]}{E_x^2} - \frac{d^2M_x}{dz_1^2}\frac{\int_{-z_0}^{z_1} E_x\, dz}{(z_1 + w)E_x} - \frac{dM_x}{dz_1} \times \left[\frac{E_x^2 - \frac{dE_x}{dz_1}\int_{-z_0}^{z_1} E_x\, dz}{(z_1 + w)E_x^2} - \frac{\left(1 + \frac{dw}{dz_1}\right)\int_{-z_0}^{z_1} E_x\, dz}{(z_1 + w)^2 E_x}\right] \qquad (7)$$

This can be rearranged to give

$$\frac{1}{E_x}\frac{d\sigma_{ix}}{dz_1} - \frac{\sigma_{ix}}{E_x^2}\frac{dE_x}{dz_1} = \frac{1}{(z_1 + w)E_x}\frac{d^2M_x}{dz_1^2} + \frac{1}{E_x}\frac{dM_x}{dz} \times \left[\frac{2}{(z_1 + w)}\frac{E_x}{\int_{-z_0}^{z_1} E_x\, dz} - \frac{1}{(z_1 + w)^2} - \frac{1}{(z_1 + w)E_x}\frac{dE_x}{dz_1}\right] \qquad (8)$$

This in turn can be written as

$$\frac{d}{dz_1}\left(\frac{\sigma_{ix}}{E_x}\right) = \frac{d}{dz_1}\left[\frac{1}{(z_1 + w)E_x}\frac{dM_x}{dz_1}\right] + \frac{1}{(z_1 + w)\int_{-z_0}^{z_1} E_x\, dz}\frac{dM_x}{dz_1} \qquad (9)$$

Noting that for a self-stressed body in which internal

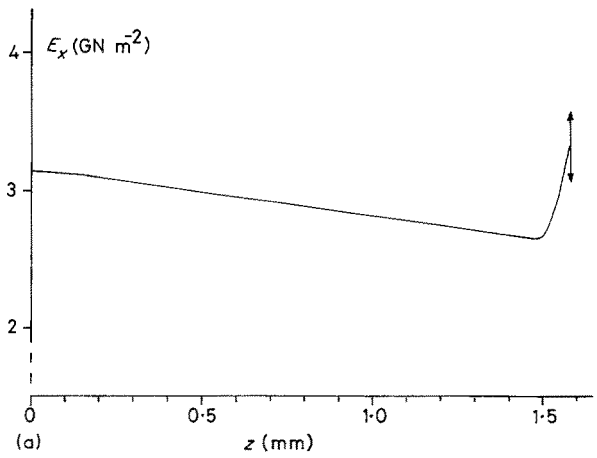

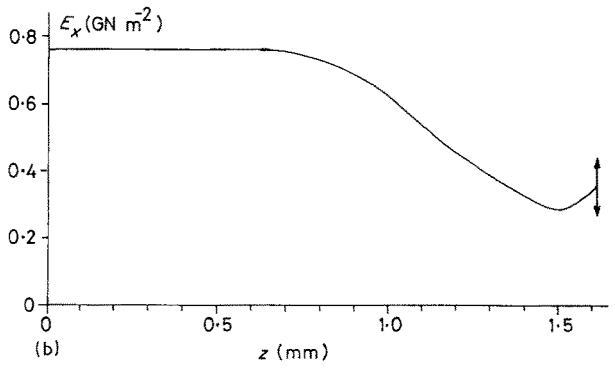

Figure 2 Young's modulus distributions for (a) dry Nylon 6, 6 bars, and (b) wet Nylon 6, 6 bars. The left-hand axis coincides with the bar centre and the surface is indicated by the vertical arrow.

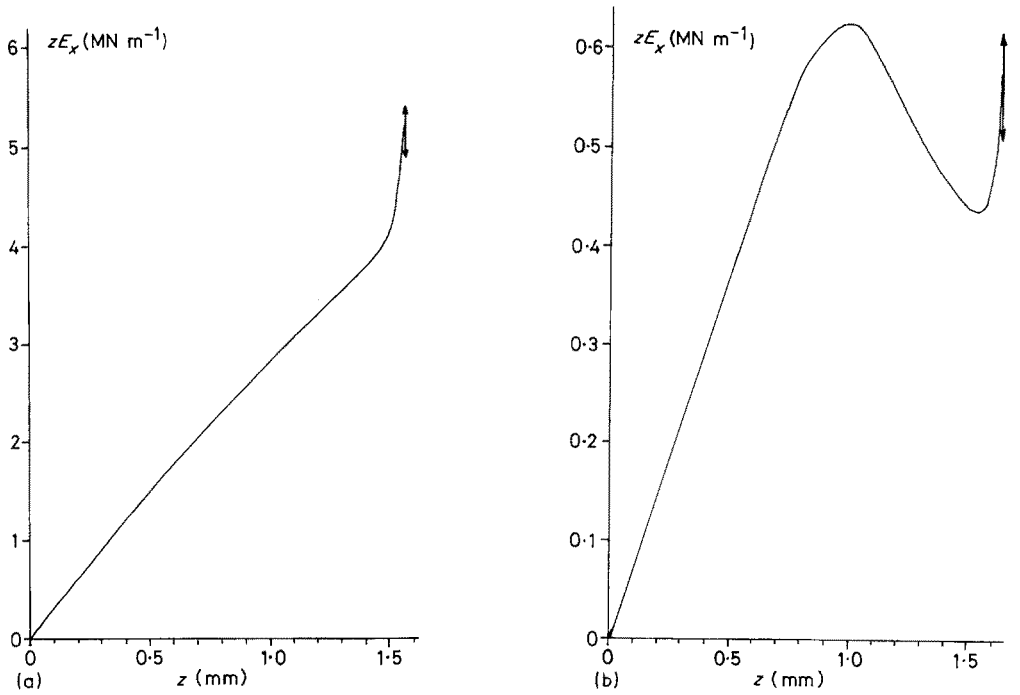

Figure 3 Plots of zE_x against distance z from the bar centre. (a) Dry bars, (b) wet bars.

force equilibrium is maintained $F_x(z_0) = 0$ and using Equation 3b, Equation 9 can be integrated between limits $z_1 = z_1$ and $z_1 = z_0$, giving

$$\frac{\sigma_{ix}(z_0)}{E_x(z_0)} - \frac{\sigma_{ix}(z_1)}{E_x(z_1)} = \frac{\sigma_{ix}(z_0)[z_0 + w(z_0)]}{[z_0 + w(z_0)]E_x(z_0)} - \frac{1}{[z_1 + w(z_1)]E_x(z_1)}\frac{dM_x}{dz_1} + \int_{z_1}^{z_0} \frac{\frac{dM_x}{dz_1}\,dz}{(z_1 + w)\int_{-z_0}^{z_1} E_x\,dz} \quad (10)$$

i.e.

$$\sigma_{ix}(z_1) = \frac{1}{(z_1 + w)}\frac{dM_x}{dz_1} - E_x(z_1)\int_{z_1}^{z_0} \frac{\frac{dM_x}{dz_1}\,dz}{(z_1 + w)\int_{-z_0}^{z_1} E_x\,dz} \quad (11)$$

This is the final form of the expression for σ_{ix}. The requirement now is to find a suitable expression for M_x. This is obtained by considering the bending moment required to cause curvature $\varrho_x(z_1)$ in the x-direction and $\varrho_y(z_1)$ in the direction transverse to it, where ϱ is the reciprocal of the radius of curvature. This can be written

$$M_x(z_1) = \int_{-z_0}^{z_1} (z + w)^2 \left[\frac{\varrho_x + v_y\varrho_y}{1 - v_x v_y}\right] E_x\,dz \quad (12)$$

where v_x and v_y are the Poisson's ratios for stresses applied in the x- and y- directions, respectively. The term within the brackets in the integrand is a constant for a particular value of z_1 and can be taken outside giving

$$M_x = \left[\frac{\varrho_x + v_y\varrho_y}{1 - v_x v_y}\right] \int_{-z_0}^{z_1} (z_1 + w)^2 E_x\,dz \quad (13)$$

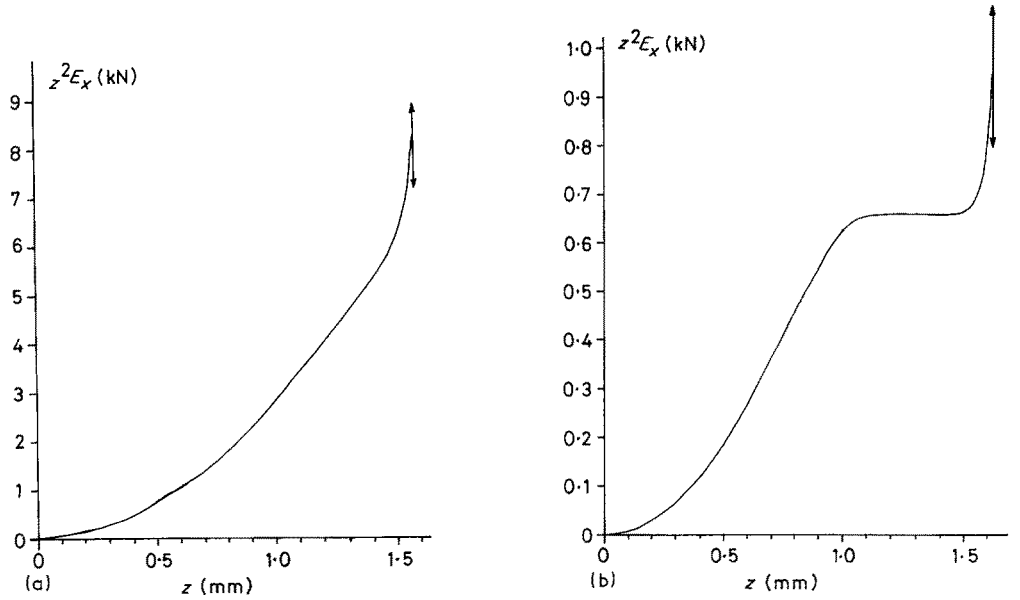

Figure 4 Plots of z^2E_x against z. (a) Dry bars, (b) wet bars.

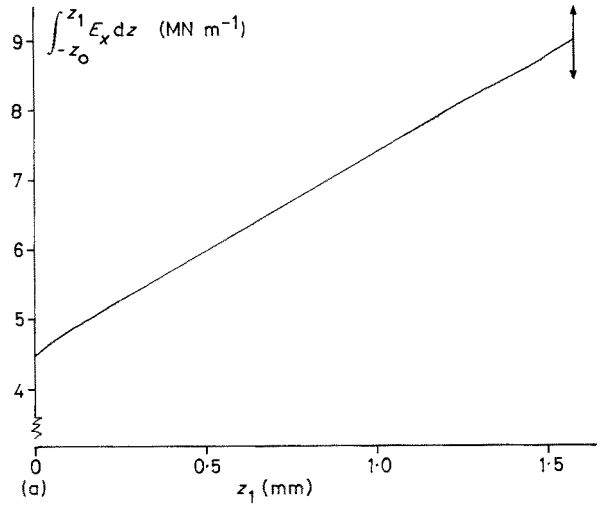

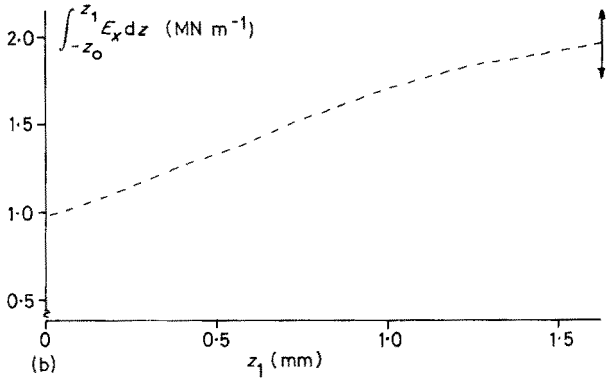

Figure 5 Plots of $\int_{-z_0}^{z_1} E_x\,dz$ against z_1. (a) Dry bars, (b) wet bars.

leading to

$$\frac{dM_x}{dz_1} = \left[\frac{\varrho_x + v_y\varrho_y}{1 - v_xv_y}\right](z_1 + w)^2E_x + \left[\frac{d\varrho_x}{dz_1} + \frac{v_y d\varrho_y}{dz_1}\right]\frac{1}{(1 - v_xv_y)} \times \left(\int_{-z_0}^{z_1} z^2E_x\,dz + 2w\int_{-z_0}^{z_1} zE_x\,dz + w^2\int_{-z_0}^{z_1} E_x\,dz\right) \quad (14)$$

If $E_x(z)$ is known, then $zE_x(z)$ and $z^2E_x(z)$ can be computed, and the integrals on the right-hand side of Equation 14 can be evaluated for selected values of z_1 by measuring areas under the plots of these functions. From Equation 1 it follows that

$$w(z_1) = -\frac{\int_{-z_0}^{z_1} zE_x\,dz}{\int_{-z_0}^{z_1} E_x\,dz} \quad (15)$$

Finally, measurements of $\varrho_x(z_1)$ and $\varrho_y(z_1)$ made at each layer removal are plotted, permitting evaluation of $d\varrho_x/dz_1$ and $d\varrho_y/dz_1$. Hence if v_x and v_y are known, dM_x/dz_1 can be obtained from Equation 14. From this the integrand in Equation 11 can be computed and plotted against z_1, and from this the integral in Equation 11 can be evaluated. Note that if Young's modulus, E_x, is uniform, then by making appropriate substitutions (e.g. $w = (z_0 - z_1)/2$) the exact form of the expression for σ_{ix} obtained by Treuting

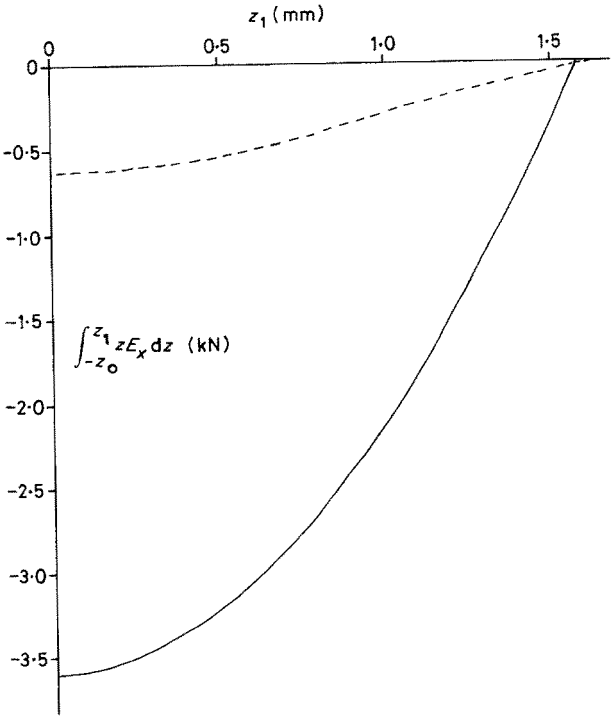

Figure 6 Plots of $\int_{-z_0}^{z_1} zE_x\,dz$ against z_1. Dry bars, solid line, wet bars, broken line.

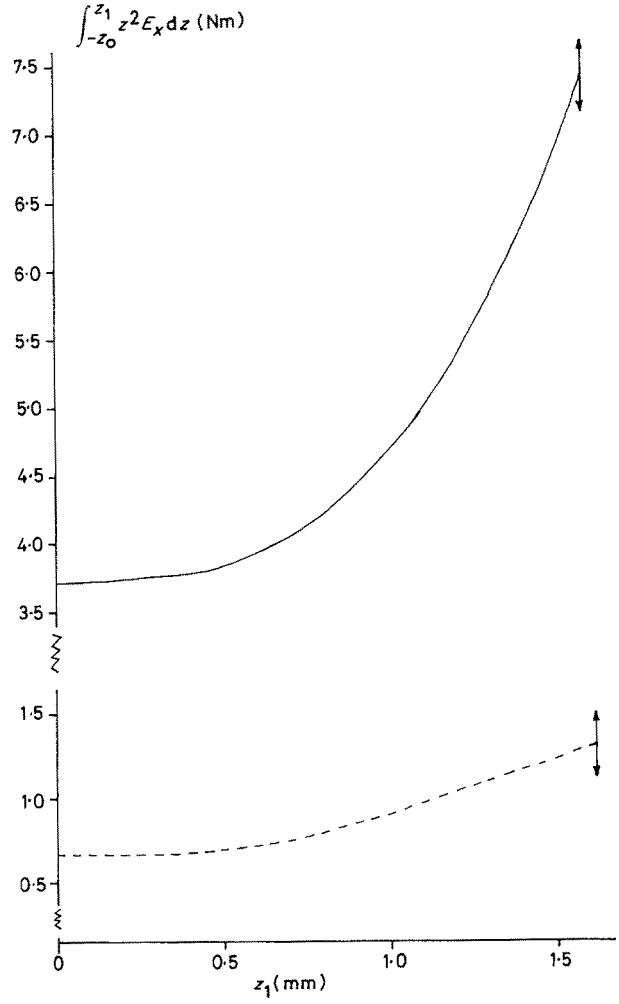

Figure 7 Plots of $\int_{-z_0}^{z_1} z^2E_x\,dz$ against z_1. Dry bars, solid line, wet bars, broken line.

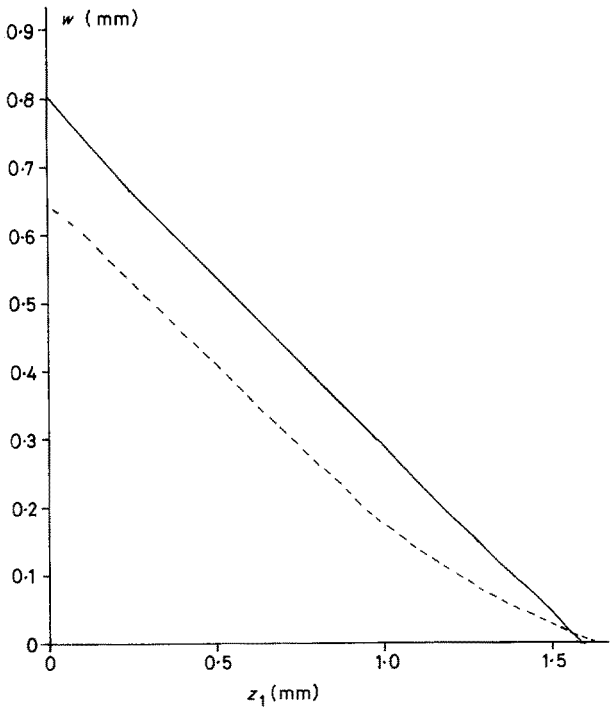

Figure 8 Plots of the displacement of the neutral surface w against the position z_1 of the top surface after layer removals. ($w = 0$ when $z_1 = z_0$). (——) Dry bars; (– – –) wet bars.

and Read is recovered from Equations 11 and 14, i.e.

$$\sigma_{ix} = \frac{E_x}{6(1 - \nu_x\nu_y)}\left\{(z_0 + z_1)^2\left[\frac{d\varrho_x}{dz_1} + \frac{\nu_y\, d\varrho_y}{dz_1}\right] + 4(z_0 + z_1)(\varrho_x + \nu_y\varrho_y) - 2\int_{z_1}^{z_0}(\varrho_x + \nu_y\varrho_y)\, dz\right\} \quad (16)$$

3. Summary and simplification of the procedure

3.1. Summary

The procedure thus reduces to the following steps:

(i) Obtain the distribution of Young's modulus with depth, $E_x(z_1)$.

(ii) Hence obtain the functions $\int_{-z_0}^{z_1} E_x\, dz$, $\int_{-z_0}^{z_1} zE_x\, dz$, $\int_{-z_0}^{z_1} z^2E_x\, dz$ and $w(z_1)$ (from Equation 15).

(iii) Measure $\varrho_x(z_1)$ and $\varrho_y(z_1)$ for successive layer removals.

(iv) Find the function $dM_x(z_1)/dz_1$ from Equation 14.

(v) Plot the function

$$Q = \frac{dM_x/dz_1}{(z_1 + w)\int_{-z_0}^{z_1} E_x\, dz} \quad (17)$$

as a function of z_1 and integrate it between the limits z_1 and z_0 for sufficient values of z_1 to generate a continuous function.

(vi) Use the results obtained above to evaluate $\sigma_{ix}(z_1)$ from Equation 11.

(vii) The stress distribution in the transverse direction, $\sigma_{iy}(z_1)$, can be evaluated using the same procedure, interchanging subscripts x and y throughout.

3.2. Simplification

It has been assumed here that ν_x and ν_y are not depth dependent. Values for ν_x and ν_y will rarely be known accurately, and it can often be assumed that $\nu_x = \nu_y$; the analysis is not very sensitive to variations in ν within the range of values commonly found to apply to thermoplastics.

In some cases the curvature in the transverse direction is small, and setting $\varrho_y = 0$ this leads to the approximate expression to replace Equation 14 as

$$\frac{dM_x}{dz_1} = \frac{\varrho_x E_x}{(1 - \nu^2)} + \frac{1}{(1 - \nu^2)}\frac{d\varrho_x}{dz_1}\left(\int_{-z_0}^{z_1} z^2E_x\, dz + 2w\int_{-z_0}^{z_1} zE_x\, dz + w^2\int_{-z_0}^{z_1} E_x\, dz\right) \quad (18)$$

The use of the approximation $\varrho_y = 0$ in the unmodified version of the Treuting and Read analysis has been discussed previously [1, 2] and its applicability in

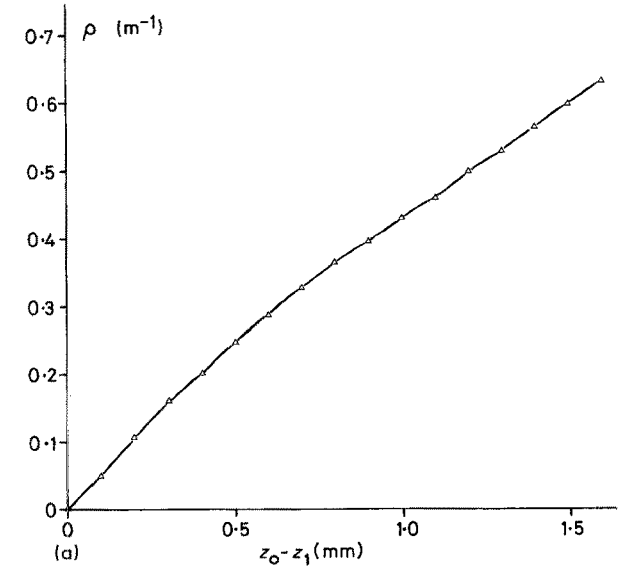

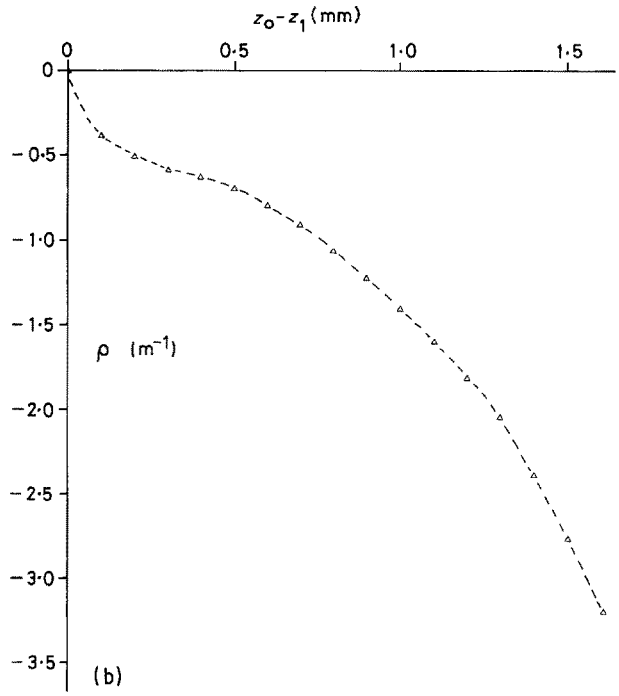

Figure 9 Curvature ϱ plotted against depth of removal ($z_0 - z_1$). (a) Dry bars, (b) wet bars.

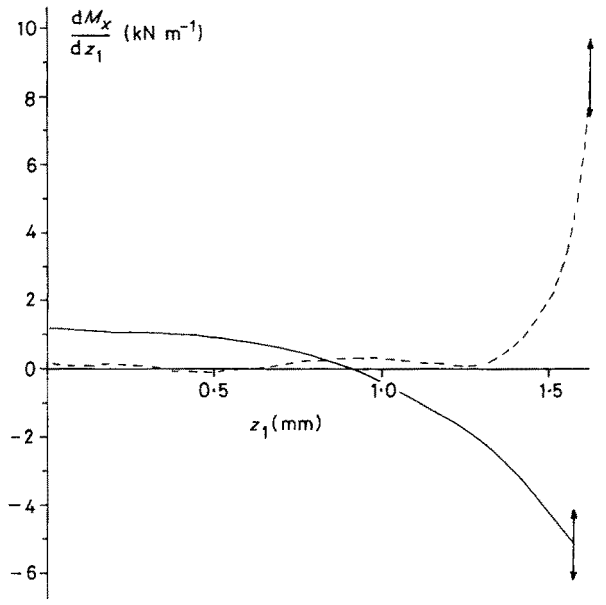

Figure 10 Plots of dM_x/dz_1 against z_1. (——) Dry bars; (– – –) wet bars.

the modified analysis presented here follows the same rules.

4. Results

To illustrate the application of this new procedure, two types of injection-moulded bar have been chosen. The first is made from nylon 6, 6 (ICI grade A100S) moulded using conventional conditions and stored in a desiccator at room temperature until used in the tests described here ("dry bars"). The second is made from the same polymer under identical conditions but stored in water at room temperature for several months, and removed just prior to testing ("wet bars"). Separate measurements confirmed that the water content of the bars stored in dry conditions was negligible, whereas those stored in water contained approximately 8% by weight of water. These particular examples were chosen for the detailed analysis presented here because they have quite different Young's modulus and residual stress distributions. The dry bars had been shown in other studies [15] to have both a fairly typical modulus distribution, varying slowly in the interior but increasing rapidly near to the surface, and a fairly conventional residual stress distribution with compressive stress near to the surface and weak tensile stresses in the interior. The wet bars have a much lower overall modulus with the maximum value at the centre, and a very different residual stress distribution, with reversed sense compared to that in the dry bar. Modulus distributions for both types of bar are shown in Fig. 2, plotted for half of the bar only; it is assumed that the distribution is symmetrical about the centre of the bar. Note that the left-hand axes in Fig. 2 coincide with the bar centre and the surface is indicated by a double-headed arrow. This point is emphasized, for later on some results are presented on graphs plotted with the left-hand axis coincident with the surface, to be consistent with earlier papers. The left-hand axis is chosen to represent the bar centre in Figs 2 to 8 and 10 to 12 because it makes the performance of the various integrations demanded by the procedure more straightforward than if it coincided with the surface. Another observation that can be made from Fig. 2 is that the wet

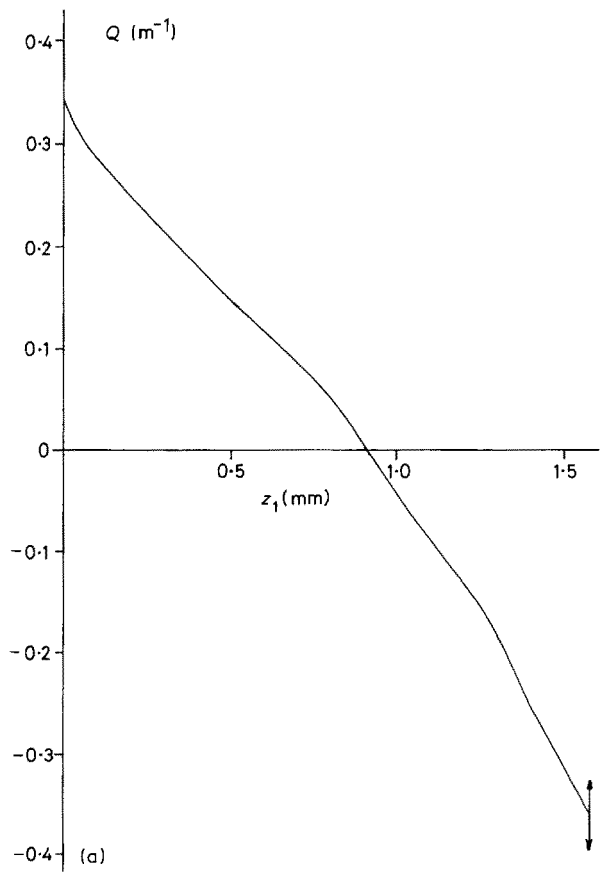

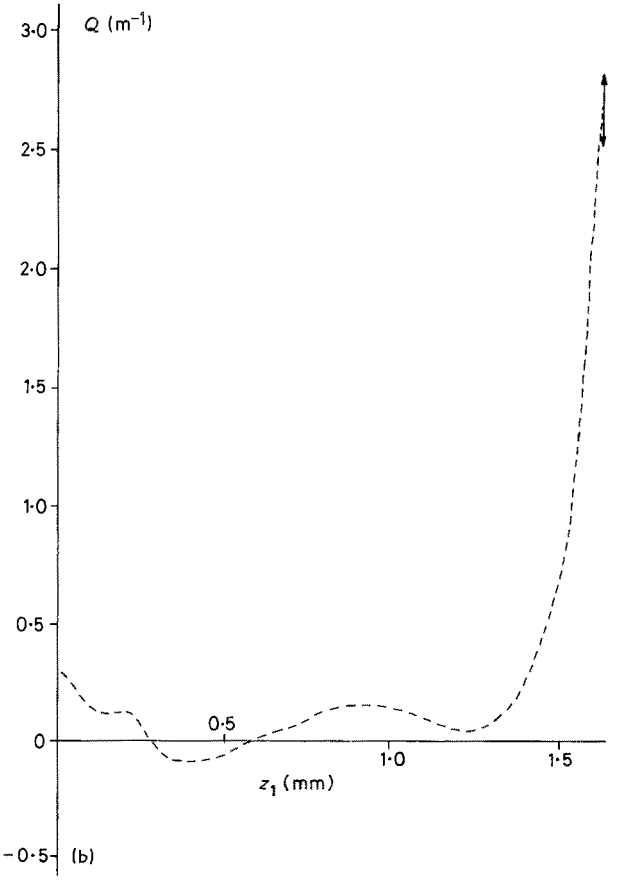

Figure 11 Plots of Q against z_1. (a) Dry bars, (b) wet bars.

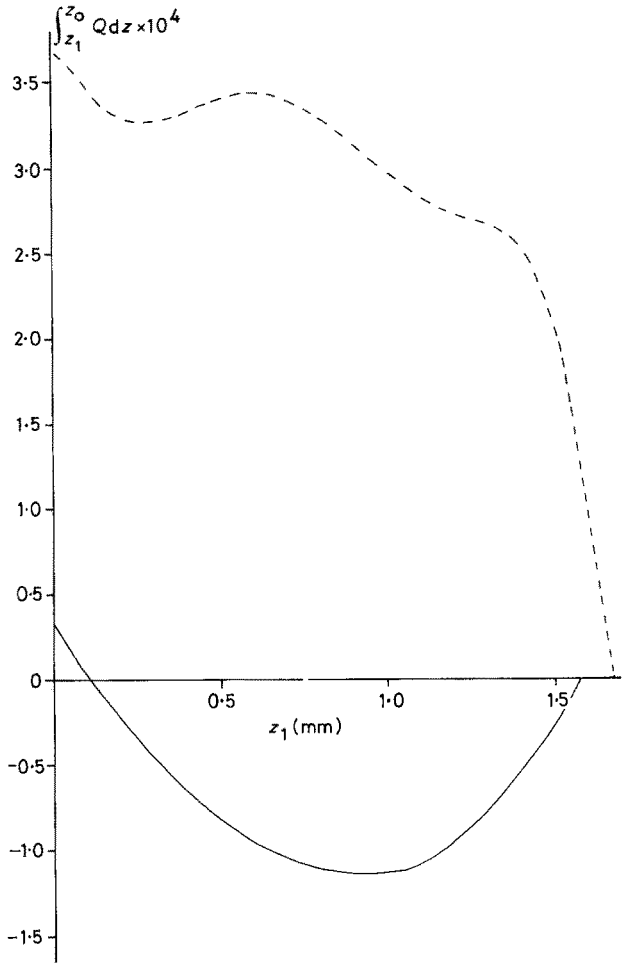

Figure 12 Plots of $\int_{z_1}^{z_0} Q\ dz$ against z_1. (——) Dry bars; (– – –) wet bars.

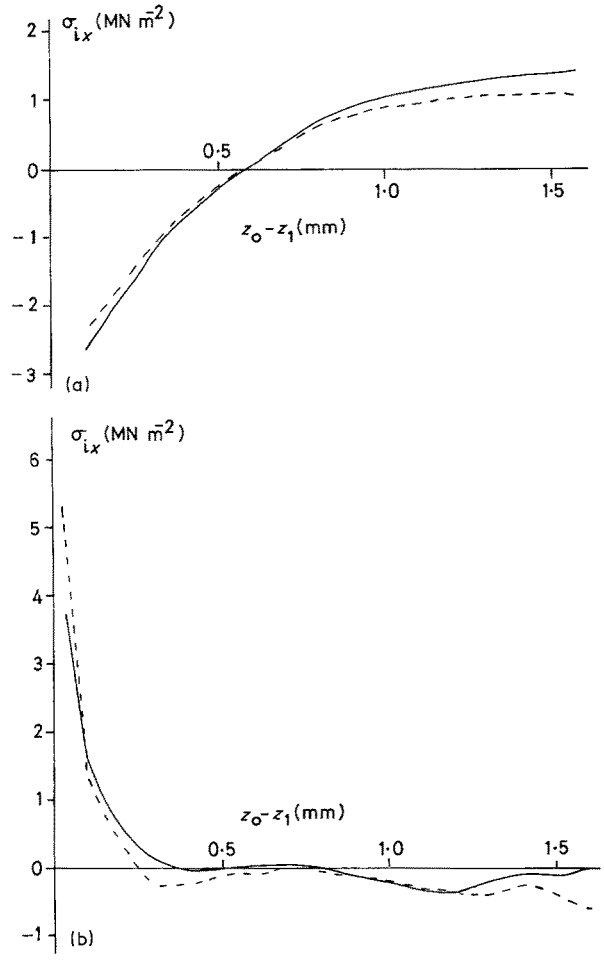

Figure 13 Residual stress distributions. (a) Dry bars, (b) wet bars. (——) Distributions obtained by the new method in which Young's modulus variations are taken into account. (– – –) Distributions obtained using the unmodified Treuting and Read analysis.

bars are considerably thicker than the dry bars as a result of swelling by the water. Further discussion of the significance of the modulus and residual stress distributions and a description of the methods used to determine the modulus distributions will be published elsewhere.

Fig. 3 shows zE_x plotted against z, again with half the bar shown and the bar surface position denoted by a vertical arrow; to obtain the full distribution note that zE_x is an odd function. Fig. 4 shows z^2E_x plotted against z; this function is even and the complete distribution is given by reflecting the graph in the vertical axis, $z = 0$. Next are presented the integrals of the functions E_x, zE_x, and z^2E_x, using as limits of integration $-z_0$ and z_1, in Figs 5, 6 and 7, respectively. Fig. 8 shows $w(z_1)$, plotted using Equation 15; the value of w falls to zero at $z_1 = z_0$. Note that it is not necessary to plot the functions shown in Figs 5 to 8; it is our reference to tabulate the functions for selected values of z_1 and to work with them in this form. The graphical method is used here simply for clarity of presentation.

Fig. 9 shows the data obtained in the layer removal tests, as curvature ϱ against $(z_0 - z_1)$; this is plotted more conventionally with the left-hand axis coincident with the bar surface. In these examples the curvature in the transverse-to-flow direction is small and the value of ϱ_y is taken to be zero. The measurements of curvature ϱ_x in the bar axis direction for successive layer removals are shown in Fig. 9 and from these plots can be obtained $d\varrho_x/dz_1$. Taking Poisson's ratio $\nu = 0.4$ the distribution dM_x/dz_1 can now be computed using Equation 18 and is shown in Fig. 10. This is used in turn with data taken from Figs 5 and 8 to obtain the expression Q given in Equation 17 and this is shown in Fig. 11. The integral of Q was evaluated between the limits z_1 and z_0 for various values of z_1 and is given in Fig. 12. Finally the residual stress distribution is computed from Equation 11 using the data in Figs 2, 8, 10 and 12 and is shown in Fig. 13 for both dry and wet bars. Shown also for comparison are the corresponding residual stress distributions obtained using the unmodified Treuting and Read analysis, taking the mean values of the distributions in Fig. 2 as the ("uniform") modulus. The general shape of the residual stress profile is preserved in both cases; there are detailed differences, but they are probably too small to be of any practical significance.

5. Discussion and conclusions

Although the procedure introduced here is rather laborious, the interpretation of the results is very straightforward. It is shown that the more exact method in which variations in Young's modulus are taken into account does not produce very large changes in the analysed profile when compared to that obtained by the conventional Treuting and Read analysis, even in the examples dealt with here in which the variations in Young's modulus through the thickness of the bars

was considerable. This was also shown in Part 1 [18]. Of much more interest than the exact stress levels is the fact that the wet bars developed tensile residual stresses near to the surface, and this result is shown equally well with the unmodified Treuting and Read analysis. These results and other observations on the effect of water uptake on Nylon 6, 6 will be discussed in a future publication. We conclude from the present study that in the majority of cases the unmodified procedure is perfectly adequate and we recommend it should continue to be the preferred method of analysis. Results presented by this laboratory and others over the past ten years or so, during which there has been considerable interest in residual stresses in polymer mouldings, are thus gauged to be generally reliable. The use of the modified procedure described for the first time here is therefore likely to be confined to cases in which the modulus variation is even more severe than in the examples used above, especially if there are sudden changes. This may occur with short-fibre-reinforced injection-moulded polymers, in which different fibre orientation distributions occur in sharply stratified layers. This type of specimen is currently under investigation.

Acknowledgements

M.W.A.P. is grateful for a studentship from SERC. The Nylon 6, 6 used for the measurements presented here was the generous gift of ICI Wilton.

References

1. B. HAWORTH, C. S. HINDLE, G. J. SANDILANDS and J. R. WHITE, *Plast. Rubb. Proc. Applic.* **2** (1982) 59.
2. J. R. WHITE, *Poly. Test.* **4** (1984) 165.
3. A. I. ISAYEV and D. L. CROUTHAMEL, *Polym. Plast. Technol. Engng* **22** (1984) 177.
4. R. G. TREUTING and W. T. READ Jr, *J. Appl. Phys.* **22** (1951) 130.
5. M. FUJIYAMA, *Kobunshi Ronbunshu* **32** (1975) 411 (English Edn. **4** 534).
6. M. FUJIYAMA and S. KIMURA, *ibid.* **32** (1975) 581 (English Edn. **4** 764).
7. *Idem, ibid.* **32** (1975) 591 (English Edn. **4** 777).
8. *Idem, J. Appl. Polym. Sci.* **22** (1978) 1225.
9. M. FUJIYAMA, H. AWAYA and S. KIMURA, *ibid.* **21** (1977) 3291.
10. M. FUJIYAMA and K. AZUMA, *ibid.* **23** (1979) 2807.
11. S. Y. HOBBS and C. F. PRATT, *ibid.* **19** (1975) 1701.
12. M. R. KAMAL and F. H. MOY, *Chem. Engng Commun.* **12** (1981) 253.
13. *Idem, Polym. Engng Rev.* **2** (1983) 381.
14. K. THOMAS, personal communication, 1981.
15. B. O'DONNELL, M. W. A. PATERSON and J. R. WHITE, unpublished results.
16. C. S. HINDLE, J. R. WHITE, D. DAWSON, W. J. GREENWOOD and K. THOMAS, SPE 39th ANTEC Boston (Society of Plastics Engineers, Brookfield Center, Connecticut, 1981) p. 783.
17. A. SIEGMANN, A. BUCHMAN and S. KENIG, *J. Mater. Sci.* **16** (1981) 3514.
18. J. R. WHITE, *ibid.* **20** (1985) 2377.

Received 8 August 1988
and accepted 11 January 1989